Supporting Information

Au Nanorod Quartets and Raman Signal Enhancement: Towards the Design of Plasmonic Platforms

Jatish Kumar,[†] Reshmi Thomas,[‡] R. S. Swathi*[‡] and K. George Thomas*[†,‡]

[†]Photosciences and Photonics, CSIR-National Institute for Interdisciplinary Science and Technology, Thiruvananthapuram 695 019, India.

[‡]School of Chemistry, Indian Institute of Science Education and Research Thiruvananthapuram (IISER-TVM), CET Campus, Thiruvananthapuram, 695016, India.

Sl.No	Table of Contents	Page No.

1. Instrumental methods and spectroscopic investigations

Solvents and reagents used were purified and dried by standard methods. Photophysical studies were carried out using spectroscopic grade solvents. The extinction spectral changes, upon the addition of the linker molecules, were recorded on a UV-visible diode array spectrophotometer (Agilent 8453). Stock solutions of the **TEGU** and the dithiols were prepared in acetonitrile. For HRTEM studies, samples were prepared by drop casting dilute solution from the cuvette on a carbon coated Cu grid and the solvent was allowed to evaporate. The specimens were examined on a FEI-Tecnai 30G^{2}S-Twin or with a 300 kV (JEOL 3010) transmission electron microscope (TEM) operated at an accelerating voltage of 300 kV. Raman spectra were recorded using a HR800 LabRAM confocal Raman spectrometer operating at 20 mW laser power using a peltier cooled CCD detector. Raman spectra were collected in a quartz cuvette using a He-Ne laser source having an excitation wavelength of 633 nm and with an acquisition time of 10 seconds using a 5x objective. All the studies were carried out in a mixture (1:4) of water and acetonitrile. The baseline was corrected and the spectra were presented after subtracting the gold nanorod spectra. No noticeable extinction spectral changes were observed for the nanorod solution during the measurements, confirming that the nanorods remain stable in solution even after exposure to laser beam.

2. Computational details

The FDTD simulations reported herein were performed using the program FDTD Solutions (version 8.5.3), a product of Lumerical Solutions, Inc. Vancouver, Canada. We use the Johnson and Christy dielectric data for modeling the frequency dependence of the dielectric constant of Au. The Au nanorods of length 55 nm and width 20 nm were used for the calculations. The gap between the nanorods was fixed as 1 nm. Water, with a refractive index

of 1.33, is chosen as the background medium. A total field-scattered field (TFSF) source of light, consisting of plane waves in the wavelength range 400−900 nm, is used as the incident beam for the simulations. We use perfectly matched layer (PML) and symmetric as well as antisymmetric boundary conditions wherever the symmetry allowed their use to save the computational time. In all our simulations, the mesh sizes are chosen by prior testing for the convergence of the numerical results.

3. Plasmon hybridization model for lateral Au nanorod dimers.

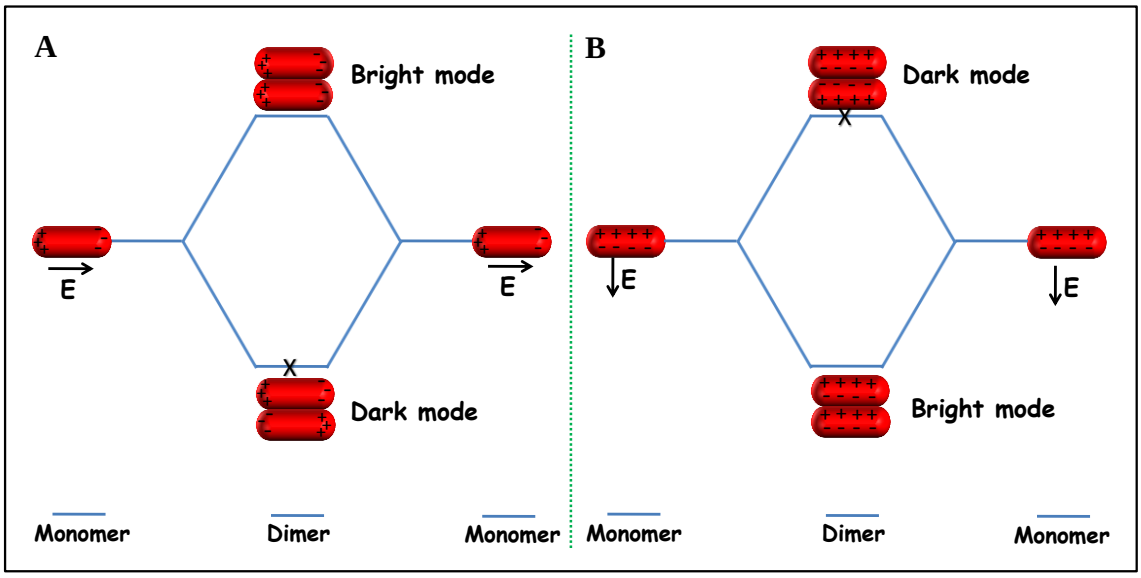

Figure S1. Illustration of the plasmon hybridization model for laterally assembled Au nanorod dimers during (A) longitudinal and (B) transverse polarizations of the incident light.

4. TEM images of nanorods at various stages of lateral assembly

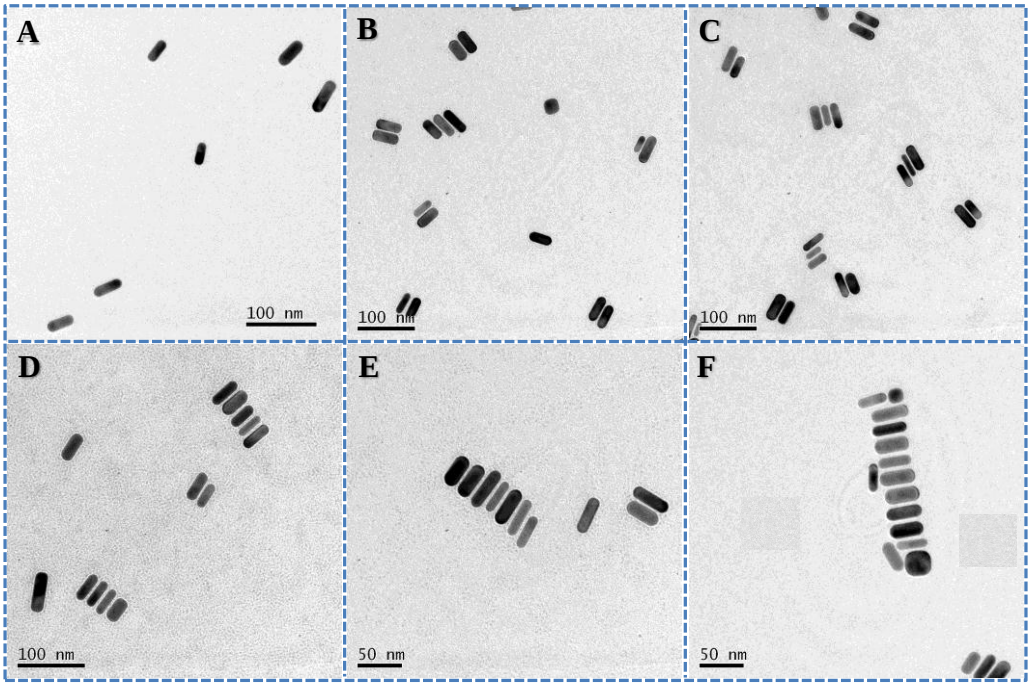

Figure S2. TEM images of gold nanorods recorded at various time intervals after the addition of 10 µM TEGU. (A) 0 min, (B) 10 min, (C) 20 min, (D) 30 min, (E) 40 min and (F) 50 min.

5. Schematic representation of CTAB bilayer on the surface of Au nanorods

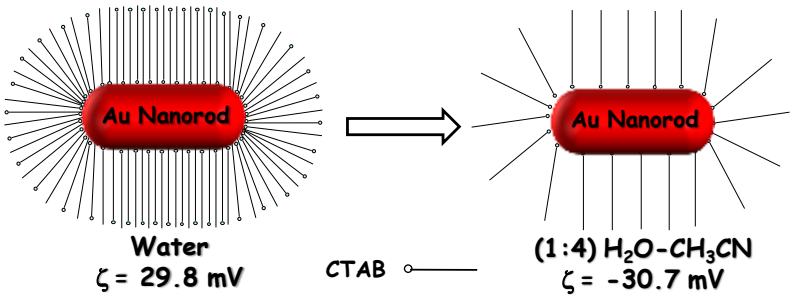

Figure S3: Schematic representation illustrating the presence of CTAB bilayer on the surface of Au nanorods in water which collapses to monolayer on changing the solvent composition to a mixture (1:4) of water and acetonitrile. This is accompanied by a reversal of ζ potential.

6. Plasmon hybridization model for lateral Au nanorod dimers of varying aspect ratio.

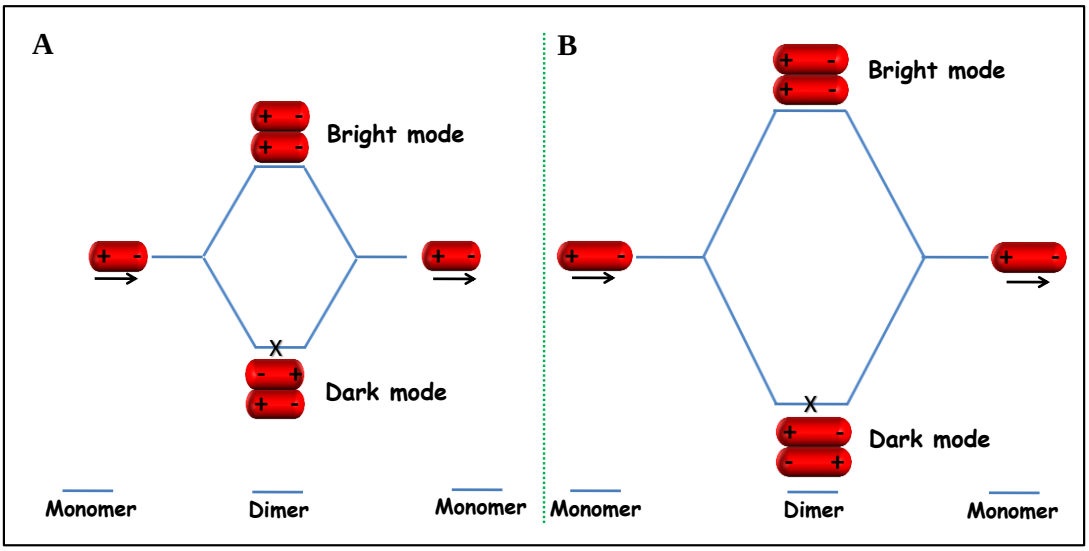

Figure S4. Illustration of the plasmon hybridization during longitudinal polarization of laterally assembled Au nanorod dimers having (A) lower aspect ratio and (B) higher aspect ratio.

7. Dependence of lateral coupling on the concentration of linker molecule

The extinction spectral changes become more pronounced and were found to be spontaneous on increasing the concentration of **TEGU** (20 µM).

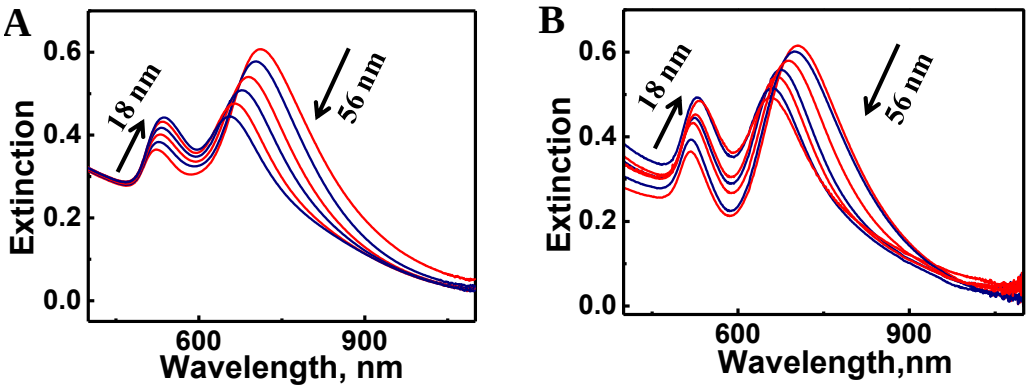

Figure S5. Extinction spectral changes of Au nanorods (0.12 nM) monitored after a time interval of (A) 45 min on addition of 10 µM and (B) 20 min on addition of 20 µM of **TEGU** in a mixture (1:4) of water and acetonitrile.

8. Lateral coupling as a function of aspect ratio of Au nanorods

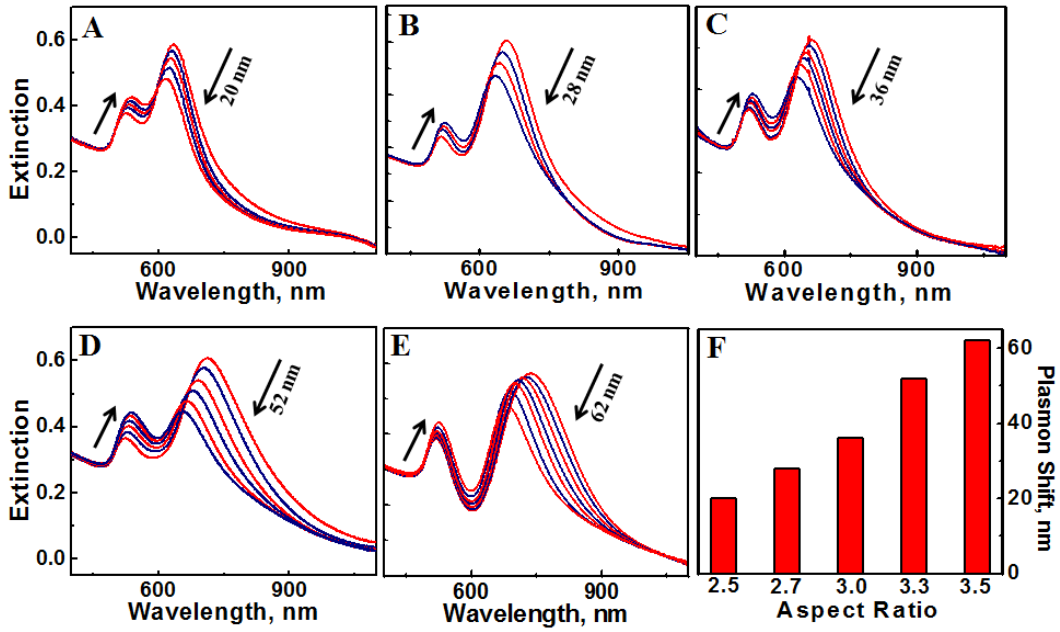

Figure S6. Extinction spectral changes on addition of **TEGU** (10 μM) in a mixture (1:4) of water and acetonitrile to Au nanorods (0.12 nM) of aspect ratio (a) 2.5, (b) 2.7, (c) 3.0, (d) 3.3, (e) 3.5. (f) Blue shift in longitudinal plasmon band plotted as a function of aspect ratio of the nanorod.

9. Extinction spectra and TEM images at different stages of quartet formation through linear assembly of lateral dimers

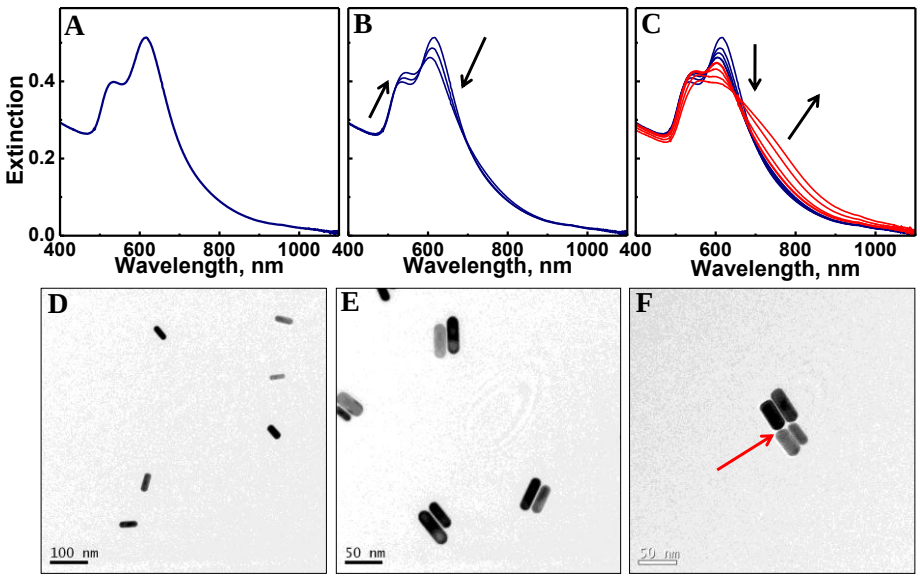

Figure S7. Extinction spectral changes (A-C) and TEM images (D-F) of Au nanorod (0.12 nM) at various stages of quartet formation. (A,D) monomers, (B,E) lateral dimers formed using **TEGU** (10 μM) as the linker and (C,F) quartets formed through the addition of 0.6 μM of **bipy-DT** (added when the extinction spectral changes correspond to the formation of lateral dimers). All studies were carried out in a mixture (1:4) of water and acetonitrile.

10. TEM images of Au nanorod quartets

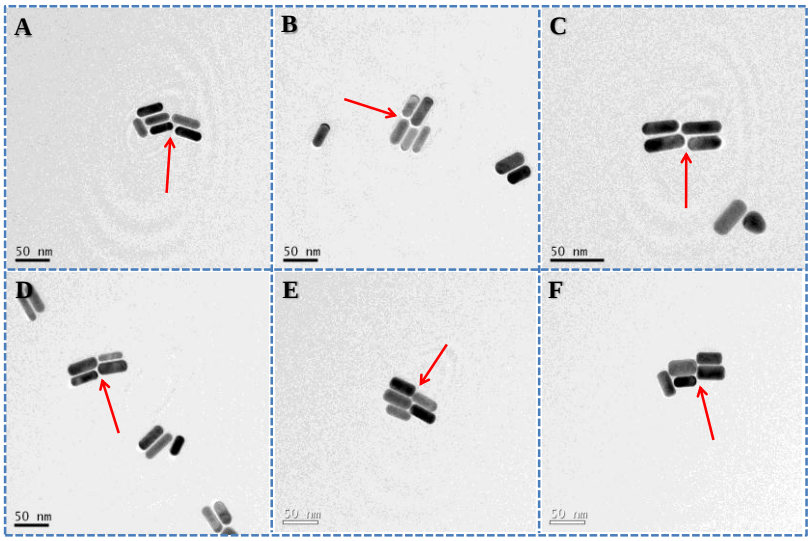

Figure S8. TEM images of Au nanorod quartets formed by the combination of lateral and longitudinal assembly processes. Images are from various locations of the grid (note: solution is dilute and hence it is difficult to locate more than one quartet in a frame after assembly).

11. Extinction spectra and TEM images at different stages of quartet formation through lateral assembly of linear dimers

The longitudinal assembly is fast and linear nanorod dimers undergo oligomerization and precipitation**.** Hence this method is not preferred.

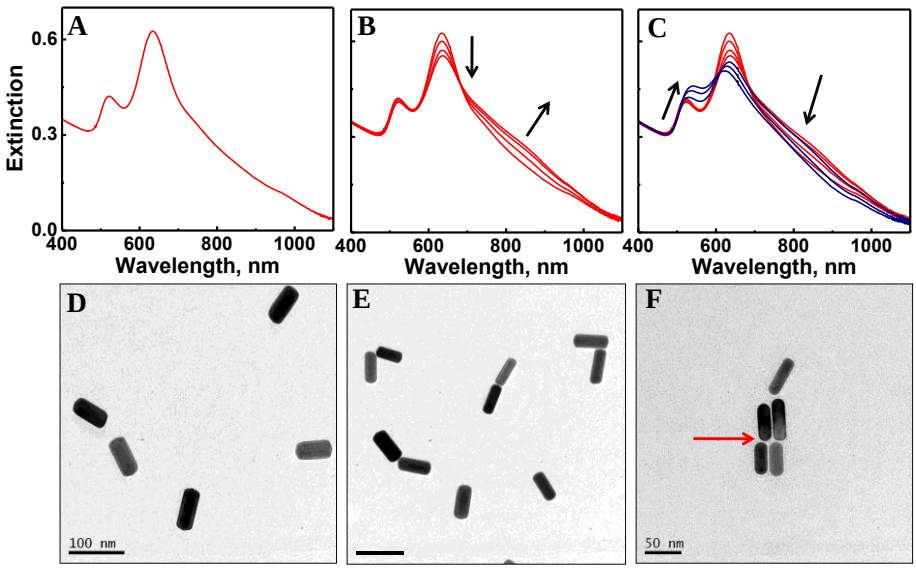

Figure S9. Extinction spectral changes (A,B,C) and TEM images (D,E,F) of Au nanorod at various stages of quartet formation. (A,D) monomers, (B,E) dimers formed using **bipy-DT** (0.6 µM) as the linker and (C,F) quartets formed through the addition of 8 µM of **TEGU** (when the spectral changes corresponds to the formation of longitudinal dimers). All studies were carried out in a mixture (1:4) of water and acetonitrile.

12. Raman spectrum of bipy-DT

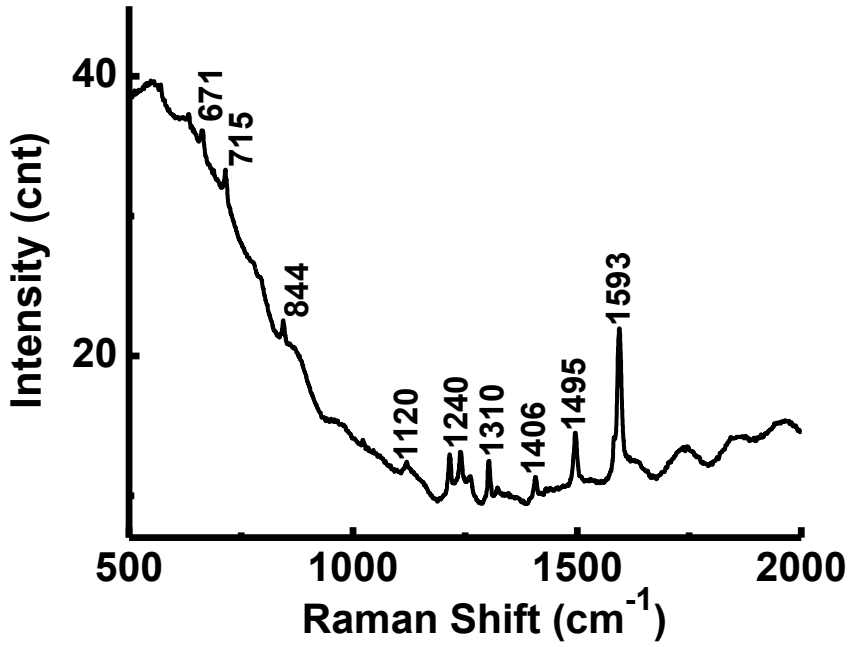

Figure S10: Raman spectrum of **bipy-DT** in the solid state

13. Assignment of Raman peaks

Table S1. Spectral data and vibrational assignment of **bipy-DT**[2,3]

SERS peaks (cm^{-1})	Assignment
687	Ring i.p. def.
715	Ring breath
856	CH o.p. bend
1156	CH i.p. def. + ring str.
1237	Inter-ring stretch + ring str. + CH i.p. def.
1320	Inter-ring str. + ring str. + CH i.p. def.
1398	CH_2 Wagging
1498	CH i.p. def. + ring str.
1598	Ring str.

i.p.: in-plane, o.p.: out-of-plane, def.: deformation, str.: stretching

14. SERS at lateral junctions of Au nanorods

A dampening in SERS intensity was observed when molecules were placed at the lateral junctions. This is due to the reduction in electric field at the lateral junctions, due to destructive interference of the surface plasmon modes

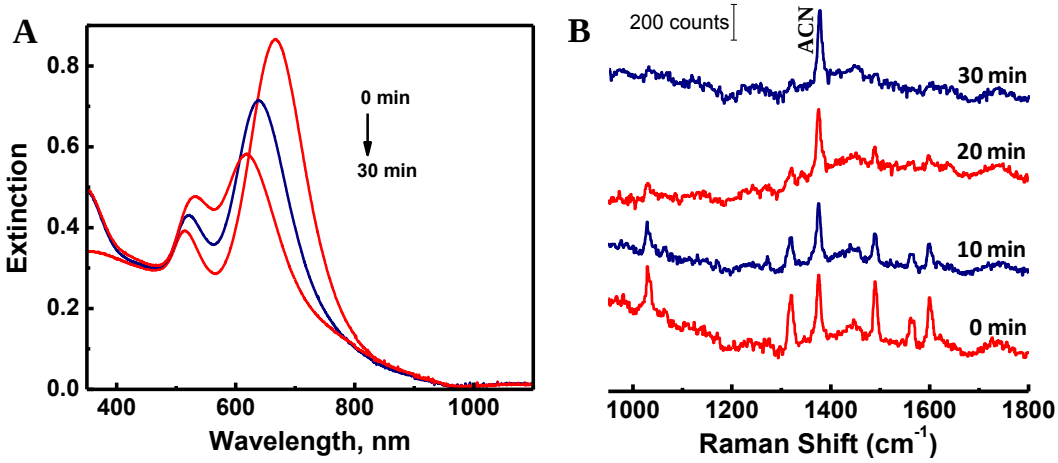

Figure S11. (A) Extinction spectral changes and (B) the SERS spectra corresponding to methyl viologen during different stages of lateral assembly of Au nanorods induced by **TEGU** (10 µM).

15. Electric field intensity distribution in the vicinity of the monomer, dimer and quartet of Au nanorods obtained using the FDTD method

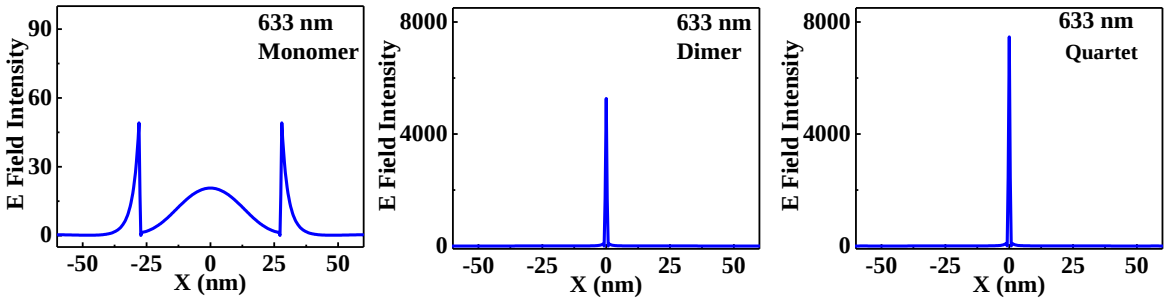

Figure S12. Plots of the electric field intensity as a function of X for the monomer, dimer and quartet of Au nanorods obtained at the laser wavelength, 633 nm. For the quartet, the field vs X data is obtained by cutting across the contour through a line passing through the centres of the two lower nanorods. Note that the incident beam is polarized along the X-axis.

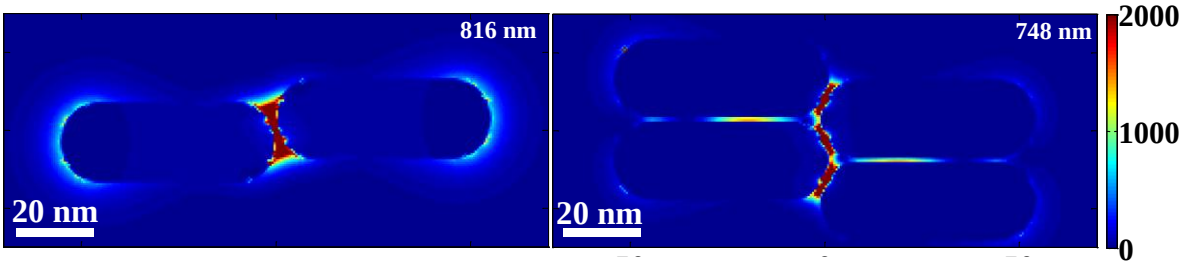

Figure S13. Contours of the electric field intensity in the vicinity of slipped dimer as well as quartet of Au nanorods at the wavelengths corresponding to their extinction maxima.

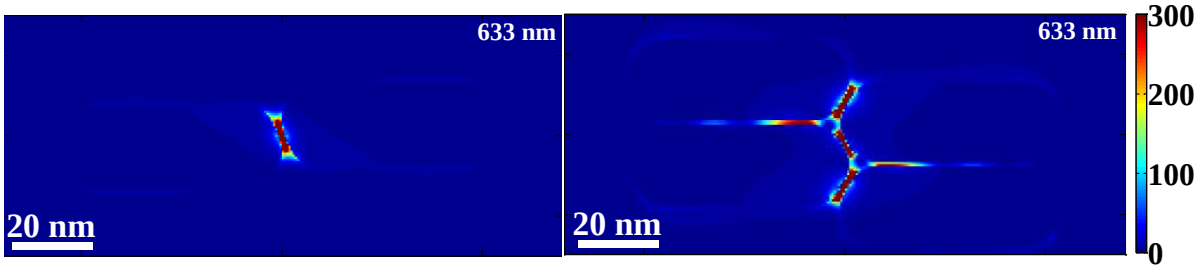

Figure S14. Contours of the electric field intensity in the vicinity of slipped dimer as well as quartet of Au nanorods at 633 nm. Note that the scale bar is chosen so as to have clarity in hot spot distribution.

16. Calculation of Enhancement Factor (EF) [4, 5]

$$\mathbf{EF = [I_{SERS}]/[I_{Raman}] \times [N_{bulk}]/[N_{ads}]}$$

I_{bulk} and I_{SERS} correspond to the intensities of the ring deformation band of dithiols in the absence and presence of Au nanorods respectively, containing various concentrations of dithiols. N_{bulk} and N_{ads} are the number of molecules probed in acetonitrile solution in the absence and presence of Au nanorods respectively.

Au nanorods possess a capsule shape having two hemispherical caps at the two ends of a cylinder and various calculations are carried by following the procedure given in our earlier reference.[6]

Total surface area of Au nanorod (length = 54.2 nm and diameter = 18.5 nm) = ~4070 nm^2

Lateral surface area of Au nanorod = ~2470 nm^2

Surface area of both edges together = ~1600 nm^2

Footprint of thiol on Au surface[6] = 0.214 nm^2

Maximum number of thiol moieties that can be accommodated on each edge of a Au nanorod = ~3740

Volume of sample probed = 168 pL

Concentration of Au nanorod = 0.12 nM

Number of nanorods in the probed volume = ~1.2 x 10^4

I) Enhancement Factor using **bipy-DT** as linker

In the absence of nanorods

Number of **bipy-DT** molecules in the probed volume (8 mM in ACN), $\mathbf{N_{bulk}}$ = ~8.08 x 10^{11}

Intensity of the ring deformation band of dithiols, **bipy-D**T (8 mM in ACN), $\mathbf{I_{bulk}}$ = 550

In the presence of nanorods

Maximum number of thiols that can be accommodated at each edge of nanorods = ~3740

Number of thiols at each edge during incubation step = ~2500 (based on rod to molecular ratio, i.e concentration of rod = 0.12 nM and thiol = 0.3 µM)

Number of thiol molecules at each edge during dimerization and quartet formation = ~3740 (based on maximum number of thiols that can be accommodated at the edges)

Number of thiols in the probed volume (adsorbed on nanorods) during incubation (0.3 µM), $\mathbf{N_{ads}}$ = ~6 x 10^7 (value corresponding to 1.2 x 10^4 rods)

Number of thiols in the probed volume (adsorbed on nanorods) during dimerization and quartet formation (0.6 µM), $\mathbf{N_{ads}}$ = ~8.9 x 10^7 (value corresponding to 1.2 x 10^4 rods)

Intensity of the ring deformation band of dithiols (**bipy-DT)** during incubation stage (0.3 µM), $\mathbf{I_{SERS}}$ = 525

Intensity of the ring deformation band of dithiols (**bipy-DT)** during the dimerization step (0.6 µM), $\mathbf{I_{SERS}}$ = 4528

Intensity of the ring deformation band of dithiols (**bipy-DT)** during the quartet formation (0.6 μM), $\mathbf{I_{SERS}}$ = 9247

EF (monomers) = $[I_{SERS}]/ [I_{Raman}]$ X $[N_{bulk}]/ [N_{ads}]$

= 525 x 8.08 x 10^{11} / 550 x 6 x 10^{7} = **1.28 x 10^{4}**

EF (dimers) = 4528 x 8.08 x 10^{11} / 550 x 8.9 x 10^{7} = **0.75 x 10^{5}**

EF (quartets) = 9447 x 8.08 x 10^{11} / 550 x 8.9 x 10^{7} = **1.55 x 10^{5}**

17. References

1. Computational Electrodynamics: The Finite-Difference Time-Domain Method, 2nd ed.; Taflove, A., Hagness, S. C., Eds.; Artech House: Norwood, MA, 2000.

2. Brolo, A. G.; Jiang, Z.; Irish, D. E. The Orientation of 2,2'-Bipyridine Adsorbed at a SERS-Active Au(111) Electrode Surface. *J. Electroanal. Chem.* **2003**, *547*, 163–172.

3. Muniz-Miranda M.; Sbrana, G. SERS-Activation of Smooth Surfaces by Doping with Silver Nanoparticles *J. Mol. Str.* 2001, **565**, 159–163.

4. Li, W.; Camargo, P. H. C.; Lu, X.; Xia, Y. Dimers of Silver Nanospheres: Facile Synthesis and Their Use as Hot Spots for Surface Enhanced Raman Scattering. *Nano Lett.* **2009**, *9*, 485–490.

5. Joseph, S. T. S.; Ipe, B. I.; Pramod, P.; Thomas, K. G. Gold Nanorods to Nanochains: Mechanistic Investigations on Their Longitudinal Assembly Using α, ω-Alkanedithiols and Interplasmon Coupling. *J. Phys. Chem. B* **2006**, *110*, 150–157.